Strong shell effects in the scattering of slow highly charged Ar ions from a Au(111) surface

W. Huang, H. Lebius, and R. Schuch
Department of Atomic Physics, Stockholm University, S-104 05 Stockholm, Sweden

M. Grether and N. Stolterfoht
Hahn-Meitner-Institut, Glienicker Strasse 100, D-14109 Berlin, Federal Republic of Germany

(Received 23 May 1997)

Slow ($E_{\mathrm{kin}}=4$ keV) highly charged Ar^{q+} ($6\leqslant q\leqslant 13$) ions were incident at 25° on a Au(111) single crystal surface. The ions scattered at an angle of 75° were analyzed in energy and charge state. When electrons are removed from the L-shell ($q\geqslant 9$) of the incoming Ar ion the yield of multiply charged scattered ions (MCSI) increases by about 3 orders of magnitude. The yield of MCSI increases monotonously with an increasing number of initial L-shell vacancies. The experimental results are compared with and interpreted by a model calculation including a side-feeding process into Ar inner shells, recapture to the surface and Auger transitions after the ion-surface interaction. [S1050-2947(97)00611-2]

PACS number(s): 34.50.Dy, 79.20.Rf

The process of neutralization of highly charged ions (HCIs) at solid surfaces has been of considerable interest in recent years. Most of the studies were performed measuring the emitted electrons and x rays [1]. The unique phenomenon that arises from these investigations is the so-called ''hollow atom'' [2–4]. Charge transfer starts at relatively large distances [5] from the metallic surface at d_c(a.u.) $\approx\sqrt{2q}/W$ (a.u.), when the potential barrier decreases below the value of the work function W, into high n levels of $n\approx q/\sqrt{2W(\text{a.u.})}$ (Ar^{9+} on Au: $d_c=22$ a.u., $n=15$). Auger cascades allow inner levels of the ''hollow atom'' to be filled if it spends a long time at the surface. These cascades can also lead to charged ions scattered from the surface.

Only a few measurements of charge state fractions of scattered HCIs from metal or quasimetallic surfaces are reported in the literature [6–9]. In these measurements an almost complete neutralization of the scattered ions was found. A small fraction of a few percent emerges at small scattering angles from the surface as charged particles. On top of that, only a weak increase (up to factor of 2) of the yield of multiply charged scattered ions is seen in these studies when an inner shell in the incoming ion is not completely filled. From the observation of the almost complete neutralization and this weak increase of charge state fractions it is concluded that, within typically 30 fs surface interaction time and many collisions with surface atoms, the inner-shell vacancies have been efficiently filled.

A motivation for the present investigation was therefore to study neutralization when highly charged ions scatter from a single surface atom. In order to make our results comparable with those for small-angle scattering, we decreased the incident velocity so that the interaction time, i.e., the time the ion spends inside a distance d_c, is of the same order of magnitude as in small-angle scattering experiments. By selecting large scattering angles and analyzing the energy of the scattered ions accurately we can ensure single collisions with surface atoms.

In these experiments we find a strong shell effect in multiply charged scattered ion (MCSI) yields. It is observed that the yield of Ar ions leaving the clean Au surface with outgoing charge states $q\geqslant 2$ increases by almost 3 orders of magnitude when the Ar ions carry initial L-shell vacancies. This result will be explained quantatively by a cascade model involving electron capture and loss and Auger processes above the crystal lattice. Dealing with single collisions avoids the difficulty in the description of neutralization in small-angle scattering that the particle undergoes several close collisions (≈ 30 [7]) with surface atoms, with varying impact parameter and distance of closest approach. It is found that in single collisions the direct inner-shell filling is not strong enough, and the interaction time is not sufficient, for inner-shell vacancies of the ions to be completely filled. In this case shell effects appear very pronounced.

The experiments were performed using the 14-GHz electron cyclotron resonance (ECR) ion source facility at the Hahn-Meitner-Institut in Berlin. Multiply charged Ar^{q+} ions ($6\leqslant q\leqslant 13$) of energy $10q$ keV were extracted from the ECR ion source and then decelerated to 4 keV ($v\approx 0.06$ a.u.) in front of the target. The incident ion beam was collimated to a diameter of about 2 mm. The beam current measured on the target was 130 nA for Ar^{9+} and was taken for on-line normalization. The ions hit a clean Au(111) single-crystal surface at $\psi=25°$ incidence angle; and scattered ions were detected at a scattering angle of $\theta=75°$. The target was mounted on an x-y-z-ψ-ϕ manipulator located in an UHV chamber with a base pressure of 3×10^{-9} mbar. The crystal was surface sputter cleaned with an Ar^{9+} beam. The surface cleanliness was verified by means of electron-induced Auger spectroscopy. The surface remained clean during the measurement due to the high incident ion current. It should be noted that the surface quality is not of the same importance in these measurements as in the aforementioned grazing incidence studies, as the interaction is localized to one or two surface atoms. The kinetic energy distributions of scattered ions in a well-defined outgoing charge state Q were measured using a tandem parallel-plate electrostatic analyzer [10] with an acceptance angle of about 1°. The overall resolution of the setup was about 5%. The energy width of scattered particles due to the finite acceptance angle is small compared to the overall resolution. The crystal orientation

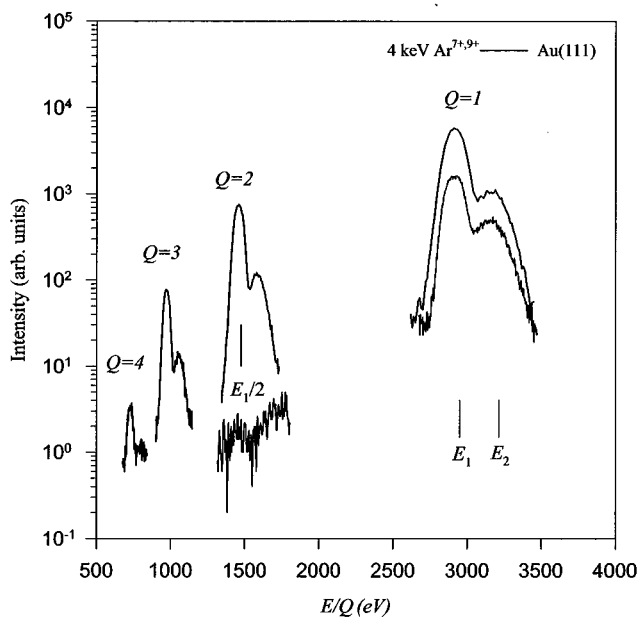

FIG. 1. Energy spectra of the scattered Ar ions for Ar^{7+} (lower lines) and Ar^{9+} (upper lines) incident at 25° on a clean Au(111) surface; q, Q, and E denote initial and final charge states of the projectiles and the energy of the scattered ions, respectively.

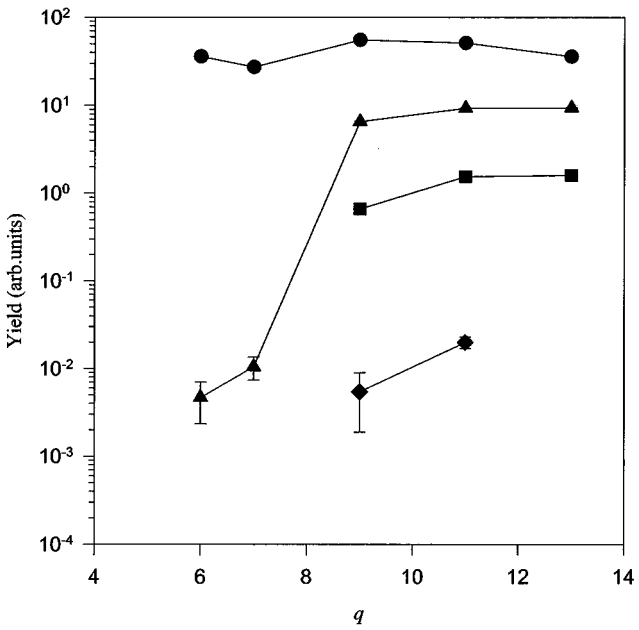

FIG. 2. Yield of scattered Ar ions with $Q=1+$(circles), $2+$(triangles), $3+$(squares), and $4+$(diamonds) obtained from 4-keV Ar^{q+} ions incident at 25° on a Au(111) surface.

with respect to the incident ion beam was determined by measuring the yield of scattered ions as a function of the azimuthal angle ϕ.

Figure 1 shows typical kinetic energy spectra obtained from primary Ar^{7+} and Ar^{9+} ions scattered off a Au(111) surface along a planar channeling direction with respect to the Au(011) crystallographic plane. The kinetic energy spectrum for each of the outgoing charge states consists of a two-peak structure: a main peak and a well-resolved smaller peak at higher energies. The main peak can be energetically assigned to Ar ions elastically scattered into the detection angle of $\theta=75°$ in a single collision with a Au atom on the surface (E_1 mark in Fig. 1). The peak at higher energy is ascribed to two sequential binary collisions with two different scattering angles with $\theta_1+\theta_2=75°$. An estimate using scattering kinematics shows that these scattering events lead to a higher final kinetic energy than the single collision events. A Marlowe simulation of scattering trajectories yields that the main contributions are found at an energy position indicated by E_2 in Fig. 1 describing a sequence of collisions with $\theta_1=18°$ and $\theta_2=57°$. We plan to describe [11] the effects of scattering trajectories and crystal orientation, i.e. the two-collision process, the influence of the extended interaction time and the occurrence of two close interactions on the neutralization of scattered ions.

For Ar^{7+} incident, mainly ions with $Q=1$ were detected. At the energy in the spectrum where scattered Ar ions with $Q=2$ are expected only a small peak was observed. The inclined background of this peak originates from the low-energy tail of Ar ions with $Q=1$. For $q\geqslant 9$, a completely different behavior of charge state distributions was observed. In contrast to the Ar^{7+} measurement, the spectra show a significant increased yield of MCSI with outgoing charge states as high as $Q=4$. It was not possible to measure $Q\geqslant 5$, because the yield was too low.

In Fig. 2 the scattered ion yields are plotted as a function of the initial charge state. Various features can be noted. The yield of singly charged scattered ions appears to be constant in this scale. For incident ions with a completely filled L shell ($q\leqslant 8$) the yield of MCSI (basically only $Q=2$ is detected) is about 3 orders of magnitude lower than that of singly charged scattered ions. However, when the incident ion carries one or more L-shell vacancies ($q\geqslant 9$) the yield of MCSI increases by nearly three orders of magnitude. This change is much higher than observed in previous measurements at small or grazing incident angles [6–9], which show a change of up to a factor of two (see discussion above). A measurement with Ar^{8+} was omitted because of metastable states ($2p^5 3s\ ^3P_{2,0}$) in the primary beam. For $q\geqslant 9$ the yield increases approximately linearly with increasing number of initial L-shell vacancies (Fig. 2).

Increasing yields of MCSI with the opening of an inner shell in the incoming ion is not very surprising as it opens the possibility of additional Auger cascades. This has already been pointed out in [6] to explain their (rather weak) charge state dependence. The astonishing facts are, on the one side, the strong increase of the yield of MCSI and, on the other side, the strong neutralization of the projectile ions. The majority (about 75%) of the scattered particles are neutral. This is very high, considering that the projectile scatters at only one Au atom on the surface. As pointed out before, in the classical over-the-barrier model the transfer of electrons starts at large distances and in high-n states. Auger cascades from these levels are too slow to fill inner-shell holes effectively, so other processes have to be found. It was seen experimentally before that inner-shell filling rates are higher than predicted for Auger cascades from high-n states [1].

A mechanism has been proposed (''side-feeding'' [12–14]) for filling inner-shell holes directly by electron transfer in close encounters of less than a few atomic units. This side

feeding is needed to describe the high neutralization (more than 90%) in grazing angle scattering [7–9]. A clear quantitative explanation with filling rates for the inner shells with large binding energies, which demonstrates that transition rates are sufficiently fast to yield this high degree of neutralization in small-angle scattering, is still missing. For large-angle scattering at a single Au atom, the integrated probability of inner-shell filling could be reduced, which would explain the observed strong shell effects. It should be pointed out that the distance of closest approach is with 1.3 a.u. for the grazing angle scattering geometry [7,9] at most a factor of 2 larger than for the large angle geometry of 0.7 a.u. [15]. The corresponding interaction times are of the same order of magnitude.

In order to verify these qualitative arguments we calculated the change of the outgoing average charge state by using a similar side-feeding model as previously employed by Winecki *et al.* [9]. We extended the model by including additionally to the filling of the Ar M-shell the N and O shells, followed by Auger cascades and recapture processes. Since cascades from high-n states give a small contribution to inner-shell filling, we assume that the contribution of all outer shells can be represented by the O-shell population.

The side-feeding rates (Γ_n^{SF}) are described by a function exponentially decaying with the distance R of the ion to the surface [9]: $\Gamma_n^{\mathrm{SF}}=\Gamma_{n0}^{\mathrm{SF}}Q\,\exp[-R/(a/2+r_n)]$, where a is the distance between two neighboring Au atoms ($a\approx 5.4$ a.u.), and Q is the average charge state of the Ar ion ($Q=18-\Sigma N_n$, N_n is the number of electrons in the shell n). A rigid theoretical justification of this formula would be useful in the future. We assume here that the Ar M shell is the lowest shell into which side feeding can occur. The electron binding energies of the M shell (e.g., $3p$ or higher) is around 20 eV. Energy matching between the Ar M shell and levels in the Au atoms is quite possible because there are many high-n states of Au in this region. However, the smallest energy gap between the Ar L-shell (e.g., $2p$) and atomic levels of Au (e.g., $4f$) amounts to 160 eV. Fast side feeding into this shell is therefore unlikely and was excluded from our model.

With electrons being transferred into M, N, and O shells, cascade processes via autoionization take place. The time-dependent populations $N_n(t)$ of the nth shell (L,M,N,O) are described by rate equations. Since transition probabilities for radiative deexcitation are at least two orders of magnitude smaller than those of Auger processes, the radiative deexcitation is omitted in the present model.

Since most of the Auger transition rates necessary for solving the rate equations are unknown, semiempirical expressions for calculating the Auger rates were used. Linear scaling weight factors are adopted instead of the quadratic factors suggested by Larkins [16]. This modification is supported by recent model calculations [4,17]. The Auger transition rates are thus given by $\Gamma^A_{n_1,n_2,n_3}(t)=\Gamma_0^{n_1,n_2,n_3}[N_{n_1,\max}-N_{n_1}(t)]\sqrt{N_{n_2}}\sqrt{N_{n_3}}\Theta_{n_2,n_3}$. Following the conventional definition of the indices used in Auger rates, n_1,n_2,n_3 stands for, e.g., LMM. The maximum number of allowed electrons in the n_1 shell is $N_{n_1,\max}$. A modified step function Θ_{n_2,n_3} was applied in order to accommodate the fact that average shell populations were used. The Auger transition rates $\Gamma_0^{n_1,n_2,n_3}$ were derived according to Ref. [18] from $\Gamma_0^{n_1,n_2,n_3}=\Gamma_0^{LMM}/\Delta n^{3.46}$, where the LMM Auger transition rate Γ_0^{LMM} can be obtained from Ref. [19] and Δn is the difference of the principal quantum numbers. With the help of this scaling rule the rates can be derived for transitions in which the two electrons involved are in the same shell (e.g., $\Gamma_0^{LMM}=\Gamma_0^{MNN}=\Gamma_0^{NOO}$). For those transitions in which the two participating electrons are not in the same initial shell, atomic structure calculations show that the rate decreases by about a factor of 3 or 9 if the electrons' principal quantum numbers differ by one or two, respectively (e.g., $\Gamma_0^{LMM}=3\Gamma_0^{LMN}$ and $\Gamma_0^{LMM}=9\Gamma_0^{LMO}$).

Near the distance of closest approach electrons from Ar N and higher shells are lost into the conduction band of Au or into empty states above the Fermi edge. For simplicity, we assume that this is described by an instantaneous charge transfer from Ar ions into Au. The model assumes that $N_n=0$ for $n=N,O$, if $r_n\geqslant R$, where $r_n=(n^2)/(Z_{\mathrm{eff}})$ and Z_{eff} being the effective charge. The projectile motion along the scattering trajectory is approximated by two straight-line trajectories with constant velocities. The velocities for incoming and outgoing trajectories are obtained from the initial energy of projectiles and the energy of the scattered ions. Energy gain by the image charge acceleration [18] ($\sim$30 eV) is neglected. The total flight time (about 1 μsec) of the ion along the trajectory is estimated according to the geometry of the experimental setup. For the initial populations the ions are assumed to be in the ground state.

The model contains three free parameters, describing the side-feeding rates $\Gamma_{n0}^{\mathrm{SF}}$ ($n=M$, N, and O), which were set equal, as our measurement presently allows only determination of one free parameter. This value was determined by the comparison between simulated and experimental values of Q for Ar^{9+}. Assuming that ions scattered from below the first atomic surface layer are totally neutralized, the average outgoing charge state for above surface scattering Q can be derived from the experimental data. We use $Q=(1+B)/(1+A)$, where A is the fraction of yields of the neutral scattered particles to the charged scattered particles that can be measured experimentally. The fraction of scattered particles below the surface to those above the surface is $B=1.8$, obtained using the Marlowe code [15].

The time evolution of L-, M-, N-, and O-shell populations is shown in Fig. 3 for Ar^{9+} and Ar^{7+}. One sees a significant difference of the occupation of L and M shells for Ar^{9+} and Ar^{7+} in the outgoing part of the trajectory. For Ar^{7+} around 90% of the M shell is filled when the ion leaves the surface, since the L shell is completely filled. Therefore, the $Q(Ar^{7+})$ can be mainly attributed to autoionization processes into the M shell. For Ar^{9+}, the L shell is not completely filled when the ions leave the surface. A significant decrease of the population in the M shell due to autoionization is seen after an interaction time of 3 fs, corresponding to a distance from the surface of 6 a.u. At this large distance, side feeding of the M shell becomes negligible. Uncompleted filling of the L shell causes, due to LMM Auger processes, a decrease of the M-shell population. Therefore the final charge state increases. The significant difference of the

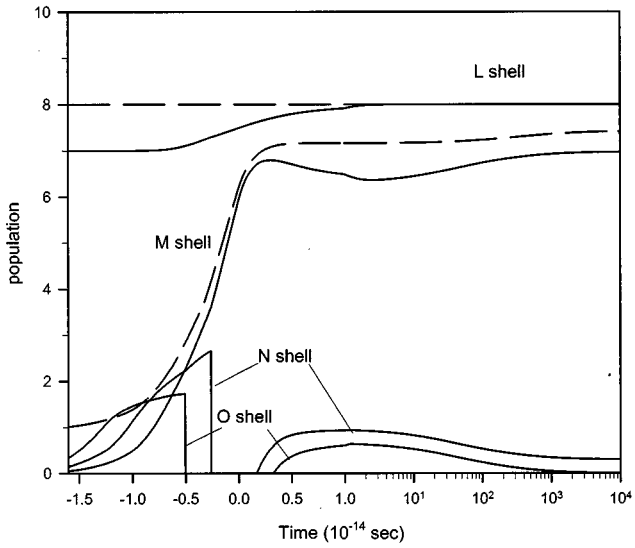

FIG. 3. Time evolution of L-, M-, N-, and O-shell populations calculated from the cascade model for 4-keV Ar^{9+} (full lines) and Ar^{7+} (dashed lines) incident at 25° on a Au(111) surface and scattered at 75°. The N- and O-shell populations for Ar^{9+} are shown only, as they do not differ significantly for Ar^{7+}.

population evolution in L and M shell for Ar^{9+} and Ar^{7+} gives rise to the strong shell effect.

With $Q(Ar^{7+})=0.26$ we got $\Gamma_{n0}^{SF}=0.012$, which is close to the value obtained in Ref. [9]. Using this parameter, the model results in the difference of the mean outgoing charge states $\Delta\overline{Q}=\overline{Q}(Ar^{9+})-\overline{Q}(Ar^{7+})=0.47$. This is in good agreement with the experimental data ($\Delta\overline{Q}=0.32\pm0.15$). However, the model overestimates $\overline{Q}$ when the incident ion has more L-shell vacancies, e.g., for $q=13$ the calculated value is $\overline{Q}=2.4$ compared to the experimental value of $\overline{Q}=0.5\pm0.2$. This disagreement may be explained by direct L-shell filling, which would contradict the above discussed assumption of supressed Ar L-shell filling due to the large energy difference to the atomic Au levels. A necessity for direct inner-shell filling has been postulated before [12–14].

In conclusion, the studies of MCSI arising from single collisions during interaction of 4-keV multiply charged Ar ions with a Au(111) surface have shown important features. First, the selection of a large scattering angle geometry results in a huge enhancement of the MCSI yield when opening an inner shell compared to the grazing angle geometry. Second, the striking difference of the shell effect between large and grazing angle collisions can be attributed to the uncompleted filling of L-shell vacancies during the ion-surface interaction. By solving rate equations for the neutralization of Ar ions in front of the surface, using side feeding, autoionization, and recapture processes, quantitative interpretations of the experimental results are given. Discrepancies with data for multiple inner-shell holes are found that point to additional direct filling of inner-shell vacancies in front of the surface.

We would like to thank S. Datz and L. Hägg for many helpful discussions. This research was supported by the Human Capital and Mobility Program under Contract No. CHRT-CT93-0103.

[1] A. Arnau, F. Aumayr, P. M. Echenique, M. Grether, W. Heiland, J. Limburg, R. Morgenstern, P. Roncin, S. Schippers, R. Schuch, N. Stolterfoht, P. Varga, T. J. M. Zouros, and HP. Winter, Surf. Sci. Rep. **27**, 113 (1997), and references therein.
[2] E. D. Donets, Phys. Scr. **T3**, 11 (1983).
[3] J. P. Briand, L. de Billy, P. Charles, S. Essabaa, P. Briand, R. Geller, J. P. Desclaux, S. Bliman, and C. Ristori, Phys. Rev. Lett. **65**, 159 (1990).
[4] N. Stolterfoht, A. Arnau, M. Grether, R. Köhrbrück, A. Spieler, R. Page, A. Saal, J. Thomaschewski, and J. Bleck-Neuhaus, Phys. Rev. A **52**, 445 (1995).
[5] J. Burgdörfer, P. Lerner, and F. W. Meyer, Phys. Rev. A **44**, 5674 (1991).
[6] S. T. de Zwart, T. Fried, U. Jellen, A. L. Boers, and A. G. Drentje, J. Phys. B **18**, L623 (1985).
[7] L. Folkerts, S. Schippers, D. M. Zehner, and F. W. Meyer, Phys. Rev. Lett. **74**, 2204 (1995).
[8] F. W. Meyer, L. Folkerts, and S. Schippers, Nucl. Instrum. Methods Phys. Res. B **100**, 366 (1995).
[9] S. Winecki, C. L. Cocke, D. Fry, and M. P. Stöckli, Phys. Rev. A **53**, 4228 (1996).
[10] A. Itoh, T. Schneider, G. Schiwietz, Z. Roller, H. Platten, G. Nolte, D. Schneider, and N. Stolterfoht, J. Phys. B **16**, 3965 (1983).
[11] W. Huang, H. Lebius, and R. Schuch (unpublished).
[12] L. Folkerts and R. Morgenstern, Europhys. Lett. **13**, 377 (1990).
[13] L. Folkerts and R. Morgenstern, Z. Phys. D **21**, 351 (1991).
[14] H. J. Andrä, A. Simionovici, T. Lamy, A. Brenac, G. Lamboley, J. J. Bonnet, A. Fleury, M. Bonnefoy, M. Chassevent, S. Andriamonje, and A. Pesnelle, Z. Phys. D **21**, 135 (1991).
[15] H. Lebius, W. Huang, and R. Schuch (unpublished).
[16] F. P. Larkins, J. Phys. B **4**, L29 (1971).
[17] R. Díez Muiño, N. Stolterfoht, A. Arnau, A. Salin, and P. M. Echenique, Phys. Rev. Lett. **76**, 4636 (1996).
[18] J. Burgdörfer and F. W. Meyer, Phys. Rev. A **47**, R20 (1993).
[19] E. J. McGuire, Phys. Rev. A **3**, 587 (1971).